Vertical displacements close to ideal-MHD marginal stability in tokamak plasmas

Fundamental Plasma Physics 5 (2023) 100017

Contents lists available at ScienceDirect

Fundamental Plasma Physics

journal homepage: www.elsevier.com/locate/fpp

Vertical displacements close to ideal-MHD marginal stability in tokamak plasmas

F. Porcelli [a,*], T. Barberis [a], A. Yolbarsop [b]

[a] Department of Applied Science and Technology, Polytechnic University of Turin, Torino 10129, Italy
[b] School of Nuclear Science and Technology, University of Science and Technology of China, Hefei, Anhui 230022, People's Republic of China

A B S T R A C T

Elongated tokamak plasmas are prone to instability, initiated by vertical displacement perturbations, which can be suppressed if a perfectly conductive wall is placed near the plasma boundary, providing passive feedback stabilization. For the more realistic case of a resistive wall, the vertical mode can still grow on the relatively slow resistive wall time scale. Active feedback control is then required for complete stabilization. However, the slow growth is far from ideal-MHD marginal stability on the stable side, i.e., provided that the wall is sufficiently close to the plasma. It is shown that the resistive growth rate can be significantly faster, scaling with fractional powers of wall resistivity, if the wall position satisfies the criterion for ideal-MHD marginal stability, thus posing more stringent conditions for active feedback stabilization.

1. Introduction

Plasma shaping and magnetic divertors have become standard in present-day tokamak experiments, as they help optimize fusion performance and reduce the adverse effects of plasma-wall interactions. On the other hand, elongated plasmas are prone to instability, initiated by an axisymmetric perturbation with toroidal mode number $n = 0$, leading to Vertical Displacement Events (VDEs) [1–4], where the entire plasma shifts vertically until it touches the vacuum chamber. Uncontrolled VDEs must be avoided, as they lead to plasma current disruptions, which can severely damage the chamber's first wall. Therefore, conducting structures are embedded in a tokamak device as a way to provide passive feedback stabilization of $n = 0$ modes, which, in the ideal magneto-hydro-dynamic (MHD) limit, would otherwise grow on Alfvén time scales, i.e., microseconds for typical experimental parameters. The passive stabilization mechanism is associated with the development of currents induced on these structures and the wall. When passive feedback stabilization is effective, active feedback stabilization, by means of currents in coils outside the vacuum chamber, is then used to suppress the residual growth on the slower time scale associated with wall resistivity, typically a few milliseconds [5,6].

Given the necessity to control the vertical instability for the safe operation of a tokamak fusion reactor, a vast amount of literature has been dedicated to the theoretical study of $n = 0$ vertical modes, starting from the pioneering work by Laval et al. [7], and continuing throughout the years (Refs. [6–16] provide a non-exhaustive sample), until very recently, where the impact of magnetic divertor X-points on $n = 0$ modes was analyzed within the framework of the ideal-MHD model [17,18]. In this article, we focus on analytic theory and consider more closely the effect of a resistive wall when the criterion for ideal-MHD stability is marginally satisfied, i.e., when the position of the wall is marginal for passive stabilization of the rapidly growing (on Alfvén time scales) $n = 0$ mode. We demonstrate that, under these conditions, the growth rate of $n = 0$ vertical displacements scales with a fractional power (smaller than unity) of wall resistivity.

More specifically, in the thin wall limit, where the wall thickness normalized to the minor radius of the elliptical wall is smaller than a certain amount, as specified in Eq. (18) below, the growth rate scales with the one-third power of resistivity. The thin wall limit is characterized by the fact that the induced currents have time to diffuse and become uniform across the thin wall. In the opposite limit of a relatively thick wall, skin currents occupy only part of the wall thickness, and the growth rate is found to scale with the one-fifth power of resistivity. In both regimes, the vertical displacement can grow on time scales that, even though much slower than the ideal-MHD Alfvén growth time, are nevertheless much faster than the resistive wall time normally considered in the design of active feedback control systems. Although the ideal-MHD marginally stable case may be somewhat special, our study indicates that there are circumstances where the active feedback control system may fail since the $n = 0$ resistive wall mode tends to grow more rapidly than normally expected.

Since the pioneering works of Coppi [19] and of Furth, Kileen and Rosenbluth [20] in 1963 on the stability of hydromagnetic systems with dissipation, it is well known that magnetized plasma equilibria close to ideal-MHD marginal stability for various types of normal modes of interest both in laboratory and in astrophysical plasmas are unstable to resistive modes with growth rates proportional to the one-third power of resistivity. Examples are interchange modes [21], internal kinks [22],

* Corresponding author.
E-mail address: francesco.porcelli@polito.it (F. Porcelli).

https://doi.org/10.1016/j.fpp.2023.100017
Received 15 January 2023; Received in revised form 1 May 2023; Accepted 5 May 2023

resistive balooning modes [23]. A fundamental aspect in these regimes is the breakdown of the so-called constant-ψ approximation, where ψ is the perturbed magnetic flux across the layer, inside the plasma, where magnetic reconnection can occur. Conversely, when the constant-ψ approximation is appropriate, tearing modes are found, whose growth rate scales with the three-fifths power of plasma resistivity [20]. However, for resistive wall modes, the situation is somewhat different. Instead of perturbed current sheets developing inside the plasma near resonant magnetic surfaces, we now have the thin wall of the plasma confinement chamber, where current sheets are induced as a consequence of nearby plasma flows. The thickness of the wall is pre-determined, and what matters in a theoretical derivation is to check whether induced currents have time to diffuse across the thin wall within the time scale of plasma motion, or whether skin currents that occupy only part of the wall thickness develop instead [24]. Standard analyses, for the relevant case where passive feedback stabilization of ideal-MHD vertical displacements is effective, consider induced currents that are uniform across the wall and growth times of the order of the resistive wall time. We show in this article that this standard result is valid only in regimes far from ideal-MHD marginality on the stable side, while close to ideal-MHD marginal stability, new possibilities arise for faster growth of resistive wall $n = 0$ modes.

This article is organized as follows. Section 2 discusses the standard case, where the resistive wall vertical displacement grows on the resistive wall time scale. Section 3 discusses the nonstandard case, close to ideal-MHD marginal stability, where growth rates scale with fractional powers of resistivity. The thin wall limit is treated in Sec. 3.1, and the induced skin current regime is treated in Sec. 3.2. A discussion of the obtained results, with numerical examples representative of typical present-day tokamak plasmas, is presented in Sec. 4. Conclusions are presented in Sec. 5. Derivations of the resistive wall stability parameter, $D_w(\gamma)$, and of the ideal wall stability parameter, D, are shown in the Appendix A. Formulas in this article are written according to c.g.s. units.

2. Axisymmetric resistive wall mode: The standard case

The first part of the derivation in this article closely follows the analysis of Ref. [25] that we summarize here for the reader's convenience. Analytic theory is possible if a relatively simple, "straight tokamak" equilibrium configuration is adopted, having periodic longitudinal length $L_z = 2\pi R_0$, where R_0 is the major radius of the equivalent torus, and equilibrium flows are absent. The plasma equilibrium current density, J_{eq}, as well as the plasma density, ρ_{eq}, are uniform up to an elliptical flux surface, with minor semi-axis a and major semi-axis b, which represents the actual plasma boundary; J_{eq} and ρ_{eq} are zero outside that boundary. The analytic solution for the equilibrium flux function in elliptical coordinates (μ, θ), where $x = A\sinh(\mu)\cos(\theta)$ and $y = A\cosh(\mu)\sin(\theta)$, with $A = \sqrt{b^2 - a^2}$, was derived in [26]. The plasma boundary is a flux surface with $\mu = \mu_b$, such that $a = A\sinh\mu_b$ and $b = A\cosh\mu_b$. The wall of the containment chamber is also assumed to be an ellipse, with b_w and a_w major and minor semi-axis, respectively. Plasma boundary and wall are assumed to be confocal, i.e., $b_w^2 - a_w^2 = b^2 - a^2$. The stability of this configuration based on the ideal MHD energy principle for a perfectly conducting wall was studied in the classic paper by Laval et al. [7]. As shown in [7,17,25], passive feedback stabilization for this plasma-wall configuration requires that magnetic X-points, associated with the elongated equilibrium, lie outside the confinement chamber, with the ideal-MHD marginal stability criterion satisfied when the wall intercepts the X-points. The "limiter plasma scenario" treated in this article is different from the "divertor plasma scenario" discussed in [17,18], where the plasma is allowed to extend to the magnetic X-points, the magnetic divertor separatrix is the actual plasma boundary, and the first wall of the vacuum chamber lies beyond the X-points.

Normal mode analysis is based on the linearized, reduced ideal-MHD (RIMHD) model [27]. A dispersion relation for $n = 0$ vertical modes was derived in [25] for arbitrary values of the ellipticity parameter,

$$e_0 = \frac{b^2 - a^2}{b^2 + a^2}. \tag{1}$$

With the help of quadratic forms, the dispersion relation takes the form $-\gamma^2\delta I = \delta W_{core}(\gamma)$. Perturbations are assumed to depend on time as $\xi \sim \exp(\gamma t)$, with $\gamma = -i\omega$ the complex eigenvalue, $\delta I = \int d^3x\rho_m\xi^2/2$, with mass density ρ_m and plasma displacement ξ, and, in the low-beta limit (beta=kinetic pressure/magnetic pressure),

$$\delta W_{core}(\gamma) = \frac{1}{2}\int d^3x\left(\mathbf{e}_z \times \frac{\nabla\tilde{\varphi}^*}{\gamma^*}\right)\ (\tilde{J}\nabla\psi_{eq} + J_{eq}\nabla\tilde{\psi}), \tag{2}$$

where an over-tilde indicates perturbed quantities, $\tilde{\varphi}^*$ is the complex conjugate of the perturbed stream function, $\tilde{\psi}$ is the perturbed magnetic flux, and $\tilde{J}$ is the perturbed current density. The volume integrals extend to the region occupied by the plasma, boundary included. δW_{core} is generally a complex, frequency-dependent quadratic form. The stabilizing effect of the wall is included in δW_{core}, as the plasma stream function is affected by the presence of the wall. Indeed, the eddy currents induced in the wall contribute to the perturbed flux, which, through the flux-freezing condition, is consistent with part of the plasma displacement, proportional to ξ_{ext}, that opposes the plasma vertical plasma shift. Indeed, as shown below, the total plasma displacement can be written as the difference between the *no-wall* displacement, ξ_∞, and this external contribution: $\xi = \xi_\infty - \xi_{ext}$.

More specifically, in the plasma region $\mu < \mu_b$, the solution of the linearized RIMHD model for the stream function in elliptical coordinates is given by

$$\tilde{\varphi}(\mu, \theta) = \gamma\,\xi\,a\frac{\sinh\mu}{\sinh\mu_b}\cos\theta, \tag{3}$$

which corresponds to a rigid vertical displacement, with the constant amplitude ξ representing the vertical shift of the plasma column. From the flux freezing condition, $\gamma\tilde{\psi} + \ \tilde{\varphi}, \psi_{eq}\big] = 0$, we obtain the corresponding perturbed magnetic flux:

$$\tilde{\psi}^-(\mu, \theta) = -\frac{\xi}{b}\frac{\cosh\mu}{\cosh\mu_b}\sin\theta, \tag{4}$$

where the subscript " - " indicates the perturbed flux in the plasma region. In the vacuum region between the plasma boundary at $\mu = \mu_b$ and the wall at $\mu = \mu_w$, the perturbed flux satisfies $\nabla^2\tilde{\psi}^+ = 0$, whose solution can be best represented as

$$\tilde{\psi}^+(\mu, \theta) = \left\{-\frac{\xi_\infty}{b}\exp\left[-(\mu - \mu_b)\right] + \frac{\xi_{ext}}{b}\frac{\cosh\mu}{\cosh\mu_b}\right\}\sin\theta, \tag{5}$$

where the subscript " + " indicates the perturbed flux in the vacuum region. In this expression, ξ_∞ is the amplitude of the rigid vertical displacement in the limit where the wall is moved to infinity, and the term proportional to ξ_{ext} represents the contribution to the perturbed flux due to the currents induced on the wall when this is at a finite distance from the plasma boundary. Continuity of flux at the plasma boundary requires that $\xi = \xi_\infty - \xi_{ext}$, so the actual vertical displacement ξ is reduced, as compared with the no-wall case, by the amount ξ_{ext}.

A straightforward derivation, detailed in [25], leads to the normalized expression for the potential energy quadratic form,

$$\delta W_{core} \propto -\frac{\pi}{2}L_z\frac{1 - a/b}{ab}\frac{1 - D_w(\gamma)}{1 - \hat{e}_0 D_w(\gamma)}\xi^2, \tag{6}$$

where $D_w = \xi_{ext}/(\hat{e}_0\xi_\infty)$, $\hat{e}_0 = e_0 b/(a + b)$, and to the dispersion relation

$$(\gamma\tau_A)^2 = \frac{4a^2b^2}{(a^2 + b^2)^2}\left(1 - \frac{a}{b}\right)\frac{1 - D_w}{1 - \hat{e}_0 D_w}, \tag{7}$$

where $\tau_A = (4\pi\varrho_m)^{1/2}/B_p'$ is the relevant Alfvén time, with $B_P{}'$ the radial derivative of the poloidal magnetic field on the magnetic axis.

Beyond the wall, the perturbed flux decays exponentially as

$$\tilde{\psi}_{out} = \psi_0\exp\left[-(\mu - \mu_w)\right]\sin\theta \tag{8}$$

The perturbed flux amplitude ψ_0 and the *resistive wall stability parameter*, $D_w(\gamma)$, are derived in the Appendix. This parameter, which in general is a function of γ, takes into account wall effects. It has the following expression:

$$D_w = \frac{\xi_{ext}}{\hat{e}_0 \xi_\infty} = D \frac{\gamma \tau_{\eta w}}{1 + \gamma \tau_{\eta w}}, \tag{9}$$

where

$$D = \frac{b^2 + a^2}{(b-a)^2} \frac{b_w - a_w}{b_w} \tag{10}$$

is a real quantity, referred to as the *ideal wall stability parameter*. As we shall see below, passive ideal wall stabilization requires vales of $D \geq 1$. The resistive wall time, $\tau_{\eta w}$, is conveniently defined as

$$\tau_{\eta w} = (\delta_w / a_w) \tau_\eta, \tag{11}$$

where $\tau_\eta = 2\pi b_w (a_w^2 + b_w^2)/[(a_w + b_w)\eta c^2]$, with c the speed of light, η the wall resistivity, and δ_w the wall thickness. Defining $\tilde{\psi}(\mu, \theta) = \hat{\psi}(\mu) \sin\theta$, a plot of the amplitude $\hat{\psi}(\mu)$ is shown in Fig. 1.

We have assumed, for the time being, that the induced current is uniform across the wall. This assumption, whose validity will be checked a posteriori, corresponds to the thin wall limit. In Sec. 3.2, this assumption will be relaxed, and attention will be given to the situation where a skin current develops, whose width is smaller than the wall thickness.

We can see from Eqs. (6),(9) and (10) that, if the wall is ideal, i.e., in the limit $\tau_{\eta w} \to \infty$, $D_w(\gamma)$ reduces to D, and δW_{core} becomes a real quantity corresponding to the usual ideal-MHD potential energy. The dispersion relation (7) with $D_w = D$ is quadratic in γ. In the limit where the wall is moved to infinity (the no-wall limit), $D \to 0$, γ^2 is positive, and ideal-MHD instability is found, with the growth rate

$$\gamma = \frac{2ab}{a^2 + b^2} \left(1 - \frac{a}{b}\right)^{1/2} \tau_A^{-1} \equiv \gamma_\infty. \tag{12}$$

Passive wall feedback stabilization requires values of $D > 1$. The maximum value, D_{max}, is always larger than unity and is reached when the wall coincides with the plasma boundary, i.e., $b_w = b$ and $a_w = a$. The ideal-MHD marginal stability criterion corresponds to $D = 1$. A calculation detailed in Ref. [25] indicates that, for the plasma equilibrium and wall geometry considered here, the marginality condition corresponds to the wall intercepting the X-points of the magnetic flux separatrix, while the unstable/stable case corresponds to the X-points lying inside/outside the vacuum chamber.

When wall resistivity is considered, the dispersion relation in the thin wall limit becomes cubic in γ:

$$\gamma^3 + \frac{\gamma^2}{(1 - \hat{e}_0 D)\tau_{\eta w}} + \gamma \gamma_\infty^2 \frac{D-1}{1 - \hat{e_0} D} - \frac{\gamma_\infty^2}{(1 - \hat{e_0} D)\tau_{\eta w}} = 0. \tag{13}$$

Let us consider the case $D > 1$, where the ideal-MHD instability is suppressed by passive feedback. The standard ordering is $\gamma_\infty \tau_{\eta w} \gg 1$ and $(D-1) = O(1)$. In this limit, two of the three roots of the cubic dispersion relation are oscillatory and weakly damped by wall resistivity,

$$\omega \approx \pm \omega_0 - i \frac{1}{2\tau_{\eta w}} \frac{D(1 - \hat{e}_0)}{(D-1)(1 - \hat{e}_0 D)}, \tag{14}$$

where $\omega_0 = \left[(D-1)/(1 - \hat{e}_0 D)\right]^{1/2} \gamma_\infty$. The third root corresponds to the weakly unstable vertical mode, growing on the resistive wall time scale:

$$\gamma \approx \frac{1}{(D-1)\tau_{\eta w}}. \tag{15}$$

Let us focus on the latter result, representing the linear growth rate for the standard $n = 0$ resistive wall mode. If we stay away from the ideal-MHD marginal stability boundary, i.e., for as long as we can take $D - 1$ positive and order unity, the dominant balance for this root involves the last two terms of the dispersion relation (13). Thus, in the linear instability phase, the vertical displacement grows on the resistive wall time, $\tau_{\eta w}$. An assumption was made for the derivation of the parameter D_w (see Appendix A), that on the mode growth time, the current induced on the wall can diffuse and become nearly uniform across the wall. Let us check this assumption. The time it takes for the induced current to diffuse across the wall of thickness δ_w can be estimated as $\tau_{diff} \sim \delta_w^2 / \eta_m$, where $\eta_m = \eta c^2 / 4\pi$ is the resistive diffusion coefficient. The induced current becomes nearly uniform across the wall if $\tau_{diff} \ll \gamma^{-1} \sim \tau_{\eta w}$. This inequality is automatically satisfied in the relevant limit $\delta_w \ll a_w$.

3. Axisymmetric resistive wall mode: The non-standard case

3.1. The thin wall limit

At ideal-MHD marginal stability, $D = 1$ and the third term of the dispersion relation (13) vanishes. In this case, and the relevant limit $\gamma_\infty \tau_{\eta w} \gg 1$, the dominant balance for the unstable root involves the first and the last term of Eq. (13), yielding

$$\gamma \approx \frac{\gamma_\infty}{(1 - \hat{e}_0)^{1/3} (\gamma_\infty \tau_{\eta w})^{1/3}} = \frac{(a_w / \delta_w)^{1/3} \gamma_\infty}{(1 - \hat{e}_0)^{1/3} (\gamma_\infty \tau_\eta)^{1/3}}. \tag{16}$$

As anticipated, the growth rate in this regime scales as the one-third power of the wall resistivity. It is considerably larger than the growth rate (15) of the standard $n = 0$ resistive wall mode (in the limit where D is positive and $D - 1 = O(1)$). In the next section, estimates of the growth rates in the standard and nonstandard regimes for typical tokamak parameters will be discussed.

The result in Eq. (16) holds for values of the parameter D close to unity. More precisely, comparing the first and the third term of Eq. (13), the width in parameter space where the result (15) holds is estimated as

$$|D - 1| \leq \frac{(1 - \hat{e}_0)^{1/3}}{(\gamma_\infty \tau_{\eta w})^{2/3}}. \tag{17}$$

Indeed, if one replaces $|D-1| \sim (1 - \hat{e}_0)^{1/3} / (\gamma_\infty \tau_{\eta w})^{2/3}$ in Eq. (15), one can see that the growth rates (15) and (16) do match.

As in the standard case, the thin wall limit corresponds to the regime where the perturbed current density induced on the wall can diffuse and become uniform across the wall on the instability growth time scale. As we have seen at the end of Sec. 2, this regime is automatically satisfied in the standard case, where the instability growth time is of the order of $\tau_{\eta w}$. For the nonstandard case treated here, the thin wall limit requires a more stringent condition of the wall thickness δ_w. The instability growth time is now estimated to be the order of the inverse of the growth rate in Eq. (16). The perturbed current density becomes uniform across the wall if $\delta_w \leq \delta_{diff} \sim (\eta_m / \gamma)^{1/2} \sim [(\delta_w / a_w)^{1/6} / (\gamma_\infty \tau_\eta)^{1/3}] a_w$, which leads to the following inequality for the wall thickness,

$$\delta_w / a_w \leq (\gamma_\infty \tau_\eta)^{-2/5}. \tag{18}$$

In these estimates, we have assumed $a_w \sim b_w$.

3.2. Induced skin currents

If the inequality (18) is not satisfied, the perturbed current induced on the wall by the vertical plasma motion does not become uniform across the wall. A skin current forms, whose width, δ_s, is less than the wall width, δ_w. In this case, our derivation of the cubic dispersion relation (13) has to be reconsidered. We can proceed as in the Appendix, but now the integral in Eq. (A4) is extended to the interval between μ_w and $\mu_w + (\delta\mu)_s$, where $(\delta\mu)_s = \delta_s / a_w$ and the subscript "s" stands for "skin". The derivation of the parameter D_w can proceed as in the Appendix, and the result is similar to that in Eq. (9), but with the important difference that $\tau_{\eta w}$ should be replaced by

$$\tau_{\eta s} = (\delta_s / a_w) \tau_\eta. \tag{19}$$

Another important difference is that, while δ_w is a given parameter representing the physical width of the wall, δ_s depends on the mode growth

rate. Therefore, its value can be determined only after the dispersion relation is solved. A good estimate for the skin depth is $\delta_s = (\ _m/\gamma)^{1/2}$. Thus, we arrive at the dispersion relation (13), with $\tau_{\eta w}$ replaced by $\tau_{\eta s} = \ _0(\tau_\eta/\gamma)^{1/2}$, $\ ^2_0 = [(1+\kappa_w^2)\kappa_w]/[2(1+\kappa_w)]$ a wall geometrical factor, and $\kappa_w = b_w/a_w$:

$$\gamma^3 + \frac{\gamma^2}{\ _0(1-\hat{e}_0 D)(\tau_\eta/\gamma)^{1/2}} + \gamma\gamma_\infty^2 \frac{D-1}{1-\hat{e_0}D} - \\ - \frac{\gamma_\infty^2}{\ _0(1-\hat{e}_0 D)(\tau_\eta/\gamma)^{1/2}} = 0. \tag{20}$$

The relevant dispersion relation is no longer cubic in γ. However, as was true in Sec. 3.1, the relevant unstable root in the limit $D = 1$ and $\gamma_\infty \tau_{\eta s} \gg 1$ can be obtained by balancing the first and the last term of Eq. (20):

$$\gamma \approx \frac{\gamma_\infty}{[\ _0(1-\hat{e}_0)]^{2/5}(\gamma_\infty \tau_\eta)^{1/5}}. \tag{21}$$

Thus, in this regime where inequality (18) is not satisfied, the growth rate scales with the one-fifth power of wall resistivity and becomes independent of the wall thickness δ_w. The growth rate (21) is larger than the growth rate (16), their ratio being of order $[(\delta_w/a_w)(\gamma_\infty\tau_\eta)^{2/5}]^{1/3}$. The two growth rates match, as they should, when $\delta_w/a_w \sim (\gamma_\infty\tau_\eta)^{-2/5}$. In these asymptotic relations, we have assumed $\ _0$ and $(1-\hat{e}_0)$ to be of order unity.

Comparing the first and the third term of the dispersion relation (20), the width in parameter space where the result (21) holds is estimated as

$$|D-1| \le \frac{1}{(\gamma_\infty\tau_\eta)^{2/5}}. \tag{22}$$

Indeed, if one replaces $\delta_w/a_w \le (\gamma_\infty\tau_\eta)^{-2/5}$ in Eq. (17), one can see that the criteria (17) and (22) do match.

It should be pointed out [28] that the thin wall limit and the induced skin current regime can be treated in a unified way following a procedure similar to that adopted in Ref. [29].

4. Discussion

It is helpful at this stage to provide some numerical estimates for the growth rates and asymptotic regimes that we have derived in this article, having in mind typical tokamak parameters.

For present-day tokamak plasmas with non-circular cross sections, taking the JET tokamak as a representative machine (see, e.g., Ref. [30]), typical parameters in S.I. units are: magnetic field, $B \sim 3$T; electron density, $n \sim 3\times10^{19}\mathrm{m}^{-3}$; ion species, Deuterium; plasma minor radius, $a \sim 1$m; elongation, $\kappa = b/a = 2$; wall distance, $b_w/b \sim 1.2 - 1.5$.

For the equilibrium model adopted in this article, the ideal wall stability parameter, Eq. (10), is a function of both κ and b_w/b:

$$D\left(\kappa, \frac{b}{b_w}\right) = \frac{\kappa^2+1}{(\kappa-1)^2}\left\{1 - \left[1 - \frac{\kappa^2-1}{\kappa^2}\left(\frac{b}{b_w}\right)^2\right]^{1/2}\right\} \tag{23}$$

In deriving Eq. (23), the confocality condition $b_w^2 - a_w^2 = b^2 - a^2$ has been used, see the Appendix for details of the algebra.

We find that the ideal-MHD marginal stability criterion, $D = 1$, is satisfied when the elliptical wall intercepts the two magnetic X-points, which, for the equilibrium model adopted in this article, are up-down symmetric and located at a vertical distance, b_X, from the magnetic axis. A simple analysis of the equilibrium configuration yields an analytic formula for b_X:

$$b_X = \frac{\kappa^2+1}{\kappa(\kappa^2-1)^{1/2}} b, \tag{24}$$

and it can be easily checked that, for $b_w = b_X$, $D(\kappa, b/b_X) = 1$. In particular, for $\kappa = 2$, $D = 1$ when $b_w = 1.4b$. Also note that, according to Eq. (23), $D < 1$, and vertical displacements are unstable whenever the X-points lie between the plasma boundary and the wall.

The fact that the ideal-MHD marginal stability criterion is exactly satisfied when the wall intercepts the X-points may be peculiar to the adopted model, where the plasma boundary and the wall are confocal ellipses. Also, real tokamak plasmas have cross-sections with a degree of triangularity, which is not considered by the present analysis. Furthermore, plasma-facing conductors are often placed inside the vacuum chamber to provide additional passive stabilization of vertical displacements. Finally, a real tokamak plasma divertor configuration is not necessarily up-down symmetric. This implies that evaluating the actual effect of the ideal wall on the stability of vertical displacements in a real experiment requires numerical work. Most importantly, the last-closed-flux-surface for a tokamak plasma with a magnetic divertor is the magnetic separatrix, where magnetic X-points lie. As pointed out in Ref. [17], since X-points are resonant to axisymmetric perturbations, $n = 0$ perturbed currents can be induced in the vicinity of the X-points and along the magnetic separatrix, which in turn may have a profound impact on vertical stability. This possibility is not taken into account in the present articles, where X-points are assumed to lie in vacuum.

With all those caveats in mind, let us consider the time scales for the growth of the resistive wall vertical displacement. The ideal-MHD growth rate, γ_∞, in the no-wall limit ($D = 0$), gives rise to a growth time in the linear instability phase of the order of the Alfvén, i.e., $\tau_\infty \sim \gamma_\infty^{-1}$ of the order of 1 μs for the typical tokamak parameters listed above. Clearly, this would be too fast to be countered by any feedback stabilization system. Fortunately, the presence of the wall provides passive feedback stabilization. According to the model adopted in this article, this requires values of $D > 1$, which are easy to satisfy if the wall is not too distant from the plasma. When $D - 1$ is positive and not too small (i.e., when inequalities (17) and (22) are not satisfied, in an asymptotic sense), the characteristic growth time of the resistive wall vertical displacement is of the order of $\tau_{\eta w} = (\delta_w/a_w)\tau_\eta$ (cf. Eq. (15). Typical values are $\tau_\eta \sim 0.1$s and $\delta_w/a_w \sim 10^{-2}$, giving rise to resistive growth times $\tau_{\eta w} \sim 1$ ms in standard regimes. This time is considerably longer than the ideal-MHD growth time. Indeed, it is long enough to allow for active feedback stabilization based on currents flowing in coils placed outside the tokamak vacuum chamber. In essence, the active stabilization system operates as follows. The vertical instability corresponds to a rigid vertical shift of the whole plasma column. An appropriate diagnostic monitors the position of the plasma centroid, which is supposed to correspond to the magnetic axis in the plasma. As soon as the centroid starts moving, currents with the appropriate sign are driven in the outer feedback coils to exert a force on the plasma that counters the vertical plasma motion. The response time of the system is limited by the electronics and is of the order of μs. A more important limiting factor is that the magnetic flux associated with the active feedback stabilization system must penetrate across the resistive wall to be felt by the plasma. The penetration time is also of the order of $\tau_{\eta w}$. Therefore, since in the standard regime, the vertical instability does not grow on a time scale much shorter than the resistive wall time, active feedback stabilization based on currents flowing in external coils can be effective.

However, near ideal-MHD marginal stability, $D \approx 1$, the resistive wall vertical displacement can grow much faster. Let us first estimate the growth rate in the thin wall limit. With the parameter values declared above, $\gamma_\infty\tau_{\eta w} \sim 10^3$ and, using the growth rate in Eq. (16), $\gamma^{-1} \sim 10\mu$s, definitely a growth time too fast for active feedback stabilization. The thin wall limit, Eq. (18), is marginally satisfied for the value of $\delta_w/a_w \sim 10^{-2}$ declared above, since $(\gamma_\infty\tau_\eta)^{-2/5} \sim 10^{-2}$. Indeed, the inverse growth rate in the regime where skin currents are induced on the wall, i.e., using the growth rate in Eq. (21), also gives $\gamma^{-1} \sim 10\mu$s. Whether the thin wall limit or the induced skin current regime applies in real tokamak experiments depends on a more accurate evaluation of the parameters δ_w/a_w and $\gamma_\infty\tau_\eta$.

A numerical solution of the dispersion relation (13) for values of D ranging between 0.9 and 1.1, focusing on the unstable root, is shown in

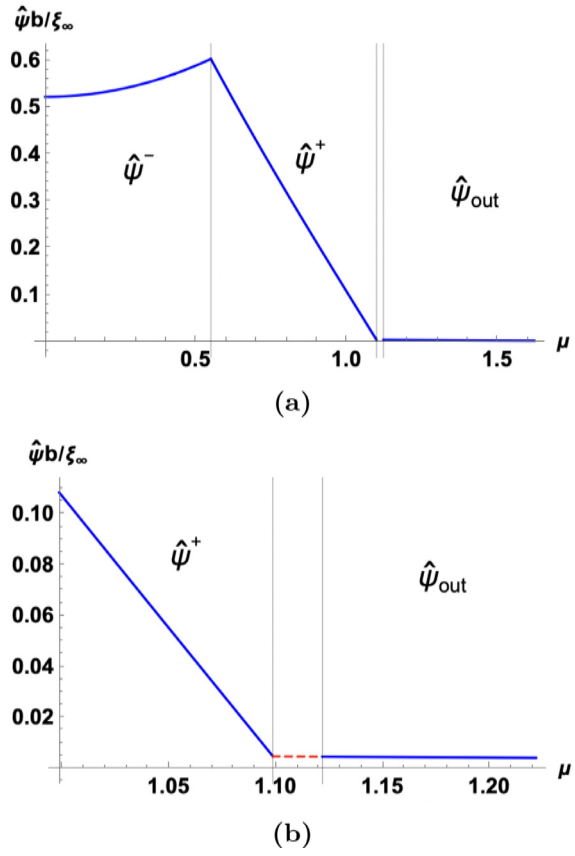

Fig. 1. Perturbed flux amplitude, $\hat{\psi}(\mu)$; 1 a shows the behaviour in the three regions, with boundaries at μ_b, μ_w and $\mu_w + \delta_w$. A zoom close to the resistive wall is shown in 1 b.

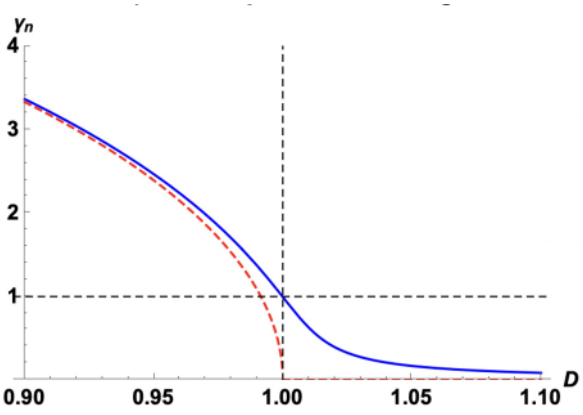

Fig. 2. Growth rate $\gamma_n = \gamma(D)/\gamma(D=1)$ for the the thin wall limit, with $\gamma(D=1)$ given in Eq. (16), as function of the ideal wall parameter D close to ideal-MHD marginal stability. The blue curve shows the numerical solution of the full cubic dispersion relation (Eq. 13), while the dashed red line represents the ideal wall solution.

Fig. 2. We can see that the inverse growth rate, i.e., the growth time in the linear instability phase, reduces rapidly and drastically as the ideal-MHD marginal stability boundary is approached. A picture showing the relative wall positions for $D = 0.9$ and $D = 1.1$ is shown in Fig. 3.

5. Conclusions

In conclusion, when the condition for ideal-MHD marginal stability for vertical displacements is satisfied, it is found that the vertical mode growth rate scales with a fractional power of resistivity. In the thin wall limit, i.e., when the wall thickness δ_w, normalized to the elliptical wall minor axis a_w, is relatively small and the inequality in Eq. (18) is satisfied, the growth rate of the vertical displacement scales with the one-third power of wall resistivity multiplied by the one-third power of the ratio a_w/δ_w, see Eq. (16). In the opposite limit, which we have dubbed the induced skin current regime, the growth rate scales with the one-fifth power of wall resistivity and becomes independent of the wall thickness, see Eq. (21). In both regimes, growth rates are considerably larger than that found in the standard regime, which scales linearly with wall resistivity, see Eq. (15). Growth rates near ideal-MHD marginal stability are too large to be countered by the active feedback stabilization system. We conclude that stable tokamak operation requires the condition for passive wall stabilization, i.e., $D > 1$ according to the model in this article, to be well satisfied. If the ideal wall stability parameter D is only slightly above unity, in the sense that either Eq. (17) in the thin wall limit, or Eq. (22) in the induced skin current regime, is satisfied, then the mode growth rate becomes considerably larger and the active feedback stabilization system can no longer be effective.

Even though growth rates scaling with fractional powers of plasma resistivity for resistive instability leading to magnetic reconnection are well known, we believe this is the first time resistive wall modes are shown to grow with fractional powers of wall resistivity in regimes that are close to ideal-MHD marginal stability.

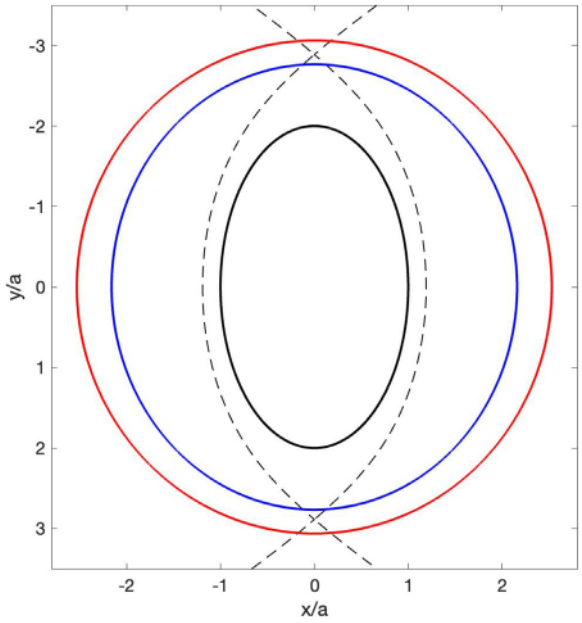

Fig. 3. Plasma boundary for $\kappa = 2$ (black curve) and relative wall positions for $D = 0.9$ (blue) and $D = 1.1$ (red). The dashed black line represents the magnetic separatrix.

Aims & scope statement

The present manuscript presents significant progress towards solving a critical problem on the stability of magnetically confined plasma, i.e., the rapid growth of resistive wall axisymmetric modes in tokamak plasmas. The article is of potential interest to a broad readership of plasma physicists, including space and laboratory plasma experts.

Declaration of Competing Interest

The authors declare that they have no known competing financial interests or personal relationships that could have appeared to influence the work reported in this paper.

CRediT authorship contribution statement

F. Porcelli: Conceptualization, Formal analysis, Investigation, Methodology, Writing – original draft, Writing – review & editing. **T. Barberis:** Formal analysis, Investigation, Methodology, Writing – review & editing. **A. Yolbarsop:** Formal analysis, Investigation, Methodology, Writing – review & editing.

Data availability

No data was used for the research described in the article.

Acknowledgements

The authors acknowledge useful discussions with Prof. Richard Fitzpatrick (IFS, University of Texas at Austin, USA) and with Prof. Francesco Pegoraro (University of Pisa, Italy).

This work has been carried out within the framework of the EUROfusion Consortium and has received funding from the Euratom Research and Training Programme (Grant Agreement No 101052200 EUROfusion). Views and opinions expressed are, however, those of the authors only and do not necessarily reflect those of the European Union or the European Commission. Neither the European Union nor the European Commission can be held responsible for them.

This work was partially supported by the National Natural Science Foundation of China under Grant No.11775220 and the National Magnetic Confinement Fusion Energy Development Program of China under Grant No.2017YFE0301702.

Appendix A. Derivation of the resistive and ideal wall parameters, D_w) and D $\kappa, b/b_w$)

The perturbed flux function in the vacuum region, $\mu_b < \mu < \mu_w$, can be written as $\tilde{\psi}^+(\mu,\theta) = \hat{\psi}(\mu)\sin\theta$, see Eq. (5). Beyond the wall, the perturbed flux function decays exponentially as

$$\tilde{\psi}_{out}(\mu,\theta) = \psi_0 e^{-(\mu-\mu_w)}\sin\theta \qquad \text{for } \mu \geq \mu_w + (\delta\mu)_w, \tag{A1}$$

where $(\delta\mu)_w$ is a small parameter, and the wall corresponds to values of μ between μ_w and $\mu_w + (\delta\mu)_w$. Since $b_w = A\cosh\mu_w$, $a_w = A\sinh\mu_w$, and $b_w + \delta_w = A\cosh[\mu_w + (\delta\mu)_w]$, expanding the latter expression for small $(\delta\mu)_w$ provides an expression for the wall thickness in physical dimensions: $\delta_w = (\delta\mu)_w a_w$.

Figure 1 is a sketch of the amplitude of the perturbed flux $\hat{\psi}(\mu)$ across the wall. Two conditions at the wall determine the parameter ψ_0 and the function $D_w(\gamma)$. The first condition is continuity of flux at the wall, $\tilde{\psi}^+(\mu_w,\theta) = \tilde{\psi}_{out}(\mu_w,\theta)$, which gives

$$\psi_0 = -\frac{\xi_\infty}{b}e^{-(\mu_w-\mu_b)} + \frac{\xi_{ext}}{b}\frac{\cosh\mu_w}{\cosh\mu_b}. \tag{A2}$$

The second condition involves the current flowing inside the wall. Consider the resistive Ohm's law for the perturbed magnetic flux within the wall, $\partial\psi_w/\partial t = (\eta c^2/4\pi)\nabla^2\psi_w$, where η is the wall resistivity. Since the wall is relatively thin, we can approximate $\partial^2\tilde{\psi}/\partial\mu^2 >> \partial^2\tilde{\psi}/\partial\theta^2$, and so

$$\frac{1}{h^2}\frac{\partial^2\hat{\psi}_w}{\partial\mu^2} = \frac{4\pi}{\eta c^2}\gamma\hat{\psi}_w, \tag{A3}$$

where $h = 1/|\nabla\mu| = 1/|\nabla\theta|$ is a scale factor. Strictly speaking, h depends on μ and θ, as $h^2 = A^2(\cosh 2\mu + \cos 2\theta)/2$. However, within the wall, $\cosh 2\mu_w = e_w^{-1}$, where $e_w = (b_w^2 - a_w^2)/(b_w^2 + a_w^2)$ is the wall ellipticity. Assuming e_w to be small, we can neglect the term $\cos 2\theta$ and approximate $h^2 \approx h^2(\mu_w) = (b_w^2 + a_w^2)/2$, where the confocality condition has been used.

We integrate Eq. (A3) across the wall,

$$\int_{\mu_w}^{\mu_w+(\delta\mu)_w}\frac{d^2\hat{\psi}_w}{d\mu^2}d\mu = \int_{\mu_w}^{\mu_w+(\delta\mu)_w} h^2\frac{4\pi\gamma}{\eta c^2}\hat{\psi}_w d\mu. \tag{A4}$$

Since the wall is thin, we can approximate $\hat{\psi}_w(\mu) \approx \psi_0$ in the second integral of Eq. (A4); also, $h(\mu) \approx h(\mu_w)$. After straightforward algebra, we obtain

$$\left(\frac{d\hat{\psi}_{out}}{d\mu} - \frac{d\hat{\psi}^+}{d\mu}\right)\Big|_{\mu_w} \approx \frac{4\pi\gamma}{\eta c^2}\frac{b_w^2 + a_w^2}{2}\frac{\delta_w}{a_w}\psi_0, \tag{A5}$$

or equivalently

$$-\frac{\xi_\infty}{b}e^{-(\mu_w-\mu_b)} - \frac{\xi_{ext}}{b}\frac{\sinh\mu_w}{\cosh\mu_b} = \left(1 + \frac{b_w + a_w}{b_w}\gamma\tau_{\eta w}\right)\psi_0, \tag{A6}$$

where $\tau_{\eta w}$ is defined in Eq. (11). Equations (A2) and (A6) allows us to determine the two unknowns ψ_0 and $D_w = \xi_{ext}/\hat{e}_0\xi_\infty$. We use $\cosh(\mu_w)/\cosh(\mu_b) = b_w/b$, $\sinh(\mu_w)/\cosh(\mu_b) = a_w/b$, $\exp(\mu_b - \mu_w) = (b+a)/(b_w + a_w)$, and $b^2 - a^2 = b_w^2 - a_w^2$. After straightforward algebra, we obtain

$$\psi_0 = -\frac{a+b}{a_w + b_w}\frac{\xi_\infty/b}{1 + \gamma\tau_{\eta w}}. \tag{A7}$$

and Eq. (9) for D_w.

The derivation above is valid in the *thin wall limit*. In the *induced skin current regime* (see Sec. 3.2), the same derivation applies, with δ_w replaced by δ_s, which depends on the growth rate γ (see the discussion at the beginning of Sec. 3.2).

We will now present the derivation of the ideal stability parameter D as a function of the elongation $\kappa = b/a$ and of the parameter b/b_w, which measures the distance of the wall from the plasma boundary, as given by Eq. (23). First, let us rewrite D in Eq. (10) as

$$D = \frac{\kappa^2 + 1}{(\kappa - 1)^2}\left(1 - \frac{a_w}{b_w}\right). \tag{A8}$$

Then, using the confocality condition, $b^2 - a^2 = b_w^2 - a_w^2$, the following expression for a_w/b_w can be obtained:

$$\frac{a_w}{b_w} = \sqrt{1 - \frac{\kappa^2 - 1}{\kappa^2}\left(\frac{b}{b_w}\right)^2}. \tag{A9}$$

By substituting this relation into (A8), we obtain the final functional relation $D(\kappa, b/b_w)$ given by (23).

It is useful to analyze the three relevant limits for $D(\kappa, b/b_w)$.

1. In the no-wall limit, where b/b_w 0, we obtain the anticipated result, D 0. Note that, as the wall is moved further away from the plasma, it becomes more circular, b_w a_w. This is a consequence of the confocality condition.
2. In the circular plasma limit, κ 1, Equation (23) reduces to $D(\kappa, b/b_w) \sim 2(b/b_w)^2/(\kappa - 1)$. In this limit, for an ideal wall, the vertical mode is stable with an oscillation frequency $\omega_0 \sim \{2(b/b_w)^2/[1 - (b/b_w)^2]\}^{1/2}\tau_A^{-1}$, which vanishes when the wall is moved to infinity. To obtain this result, we have used the definition of ω_0 given below Eq. (14).
3. Lastly, in the limit where the wall approaches the plasma boundary, b/b_w 1, Eq. (23) reaches its maximum value (for a given elongation κ), $D(\kappa, b/b_w)$ $D_{max} = (\kappa^2 + 1)/[\kappa(\kappa - 1)]$, which is always larger than unity.

References

[1] E. Strait, L. Lao, J. Luxon, E. Reis, Observation of poloidal current flow to the vacuum vessel wall during vertical instabilities in the DIII-D tokamak, Nucl. Fusion 31 (3) (1991) 527–534, doi:10.1088/0029-5515/31/3/011.
[2] R. Granetz, I. Hutchinson, J. Sorci, J. Irby, B. LaBombard, D. Gwinn, Disruptions and halo currents in Alcator C-Mod, Nucl. Fusion 36 (5) (1996) 545–556, doi:10.1088/0029-5515/36/5/i02.
[3] M. Albanese R. Mattei, F. Villone, Prediction of the growth rates of VDEs in JET, Nucl. Fusion 44 (2004) 999.
[4] V. Riccardo, JET EFDA Contributors, Progress in understanding halo current at JET, Nucl. Fusion 49 (2009) 055012.
[5] J.B. Lister, et al., Experimental study of the vertical stability of high decay index plasmas in the diii-d tokamak, Nucl. Fusion 30 (11) (1990) 2349, doi:10.1088/0029-5515/30/11/011.
[6] E.A. Lazarus, J.B. Lister, G.H. Neilson, Control of the vertical instability in tokamaks, Nucl. Fusion 30 (1990) 111.

[7] G. Laval, R. Pellat, J.L. Soule, Hydromagnetic stability of a currentcarrying pinch with noncircular cross section, Phys. Fluids 17 (1974) 835.
[8] M. Okabayashi, G. Sheffield, Vertical stability of elongated tokamaks, Nucl. Fusion 14 (2) (1974) 263–265, doi:10.1088/0029-5515/14/2/011.
[9] E. Rebhan, Stability boundaries of tokamaks with respect to rigid displacements, Nucl. Fusion 15 (1975) 277.
[10] E. Haas, Stability of a high-β tokamak to uniform vertical displacements, Nucl. Fusion 15 (1975) 407.
[11] M. Perrone, J. Wesson, Stability of axisymmetric modes in JET, Nucl. Fusion 21 (1981) 871.
[12] R. Fitzpatrick, A simple ideal magnetohydrodynamical model of vertical disruption events in tokamaks, Phys. Plasmas 16 (1) (2009) 012506, doi:10.1063/1.3068467.
[13] L.E. Zakharov, S.A. Galkin, S.N. Gerasimov, contributors JET-EFDA, Understanding disruptions in tokamaks, Phys. Plasmas 19 (5) (2012) 055703, doi:10.1063/1.4705694.
[14] A. Portone, Active and passive stabilization of n=0 RWMs in future tokamak devices, Nucl. Fusion 57 (2017) 126060.
[15] C.F. Clauser, S.C. Jardin, N.M. Ferraro, Vertical forces during vertical displacement events in an ITER plasma and the role of halo currents, Nucl. Fusion 59 (2019) 126037.
[16] I. Krebs, et al., Axisymmetric simulations of vertical displacement events in tokamaks: A benchmark of M3D-C1, NIMROD, and JOREK, Phys. Plasmas 27 (2020) 022505.
[17] A. Yolbarsop, F. Porcelli, R. Fitzpatrick, Impact of magnetic X-points on the vertical stability of tokamak plasmas, Nucl. Fusion 61 (11) (2021) 114003.
[18] A. Yolbarsop, F. Porcelli, W. Liu, R. Fitzpatrick, Analytic theory of ideal-MHD vertical displacements in tokamak plasmas, Plasma Phys. Contr. Fusion 64 (2022) 105002, doi:10.1088/1361-6587/ac7ee6.
[19] B. Coppi, On the stability of hydromagnetic systems with dissipation, in: Propagation and instabilities in plasmas, 7th Lockheed Symposium on Magnetohydrodynamics Palo Alto, CA, 1962, Stanford University Press, 1963, pp. 70–86.
[20] H.P. Furth, J. Killeen, M.N. Rosenbluth, Finite resistivity instabilities of a sheet pinch, Phys. Fluids 6 (1963) 459.
[21] B. Coppi, J.M. Greene, J.L. Johnson, Resistive instability in a diffuse linear pinch, Nucl. Fusion 6 (1966) 101.
[22] B. Coppi, R. Galvão, R. Pellat, M.N. Rosenbluth, P. Rutherford, Resistive internal kink modes, Sov. J. Plasma Phys. 2 (1976) 533.
[23] H.R. Strauss, Resistive ballooning modes, Phys. Fluids 24 (1981) 2004.
[24] R. Fitzpatrick, A simple model of the resistive wall mode in tokamaks, Phys. Plasmas 9 (8) (2002) 3459–3469, doi:10.1063/1.1491254.
[25] T. Barberis, A. Yolbarsop, F. Porcelli, Vertical displacement oscillatory modes in tokamak plasmas, J. Plasma Phys. 88 (5) (2022) 905880511, doi:10.1017/S0022377822000988.
[26] F. Porcelli, A. Yolbarsop, Analytic equilibrium of æstraight tokamakg plasma bounded by a magnetic separatrix, Phys. Plasmas 26 (2019) 054501.
[27] H.R. Strauss, Nonlinear, threedimensional magnetohydrodynamics of noncircular tokamaks, Phys. Fluids 19 (1976) 134.
[28] R. Fitzpatrick, private communication.
[29] B. Chapman, R. Fitzpatrick, D. Craig, P. Martin, G. Spizzo, Observation of tearing mode deceleration and locking due to eddy currents induced in a conducting shell, Phys. Plasmas 11 (5) (2004) 2156–2171, doi:10.1063/1.1689353.
[30] X. Lituadon, et al., Overview of the JET results in support to ITER, Nucl. Fusion 57 (2017) 102001.